MODELLING AND CONTROL OF GRID-CONNECTED PHOTOVOLTAIC SYSTEMS

H. BOUMAARAF, A. TALHA
Laboratory of Instrumentation, Faculty of Electronics and Computer, University of Sciences and Technology Houari Boumediene
BP 32 El-Alia 16111 Bab-Ezzouar, Algiers, Algeria, Phone: +213 21 24 79 50 – 60,
Email: boumaaraf.houria@gmail.com, abtalha@gmail.com

O. BOUHALI
[3]LAMEL Laboratory, Jijel University
BP 98, Ouled Aissa, Jijel, Algeria, Phone: +213 213 034 50 14 00, Email: bouhali_omar@yahoo.fr

Abstract: *The objective of this work is to study the performances of a photovoltaic (PV) system connected to the grid using a Voltage Source Inverter (VSI).*
To obtain the maximum power from a photovoltaic generator and to match the solar cell power to the environmental changes a DC-DC buck-boost inverter controlled by the fuzzy logic command is used.
The effectiveness of grid-connected photovoltaic power generation systems depends on the efficiency of the DC-into-AC conversion. For the grid connected inverter is desirable to provide the unity power factor. The performance of grid connected photovoltaic system using a two level inverter which can synchronise a sinusoidal current output with a voltage grid is shown by the numerical simulation.

Key words: *MPPT, Inverter, Buck-Boost, Grid, Fuzzy logic controller.*

1. Introduction

Nowadays photovoltaic energy is one of the important renewable sources, since it is clean energy source that allows for local energy independence, inexhaustible. Unlike fossil fuels, harnessing solar energy doesn't result in harmful CO_2 emissions, it have a low cost and high efficiency during energy conversion [1][2]. Regarding to this, it is necessary to optimize the performance of PV systems through the operation of conversion systems to increase the output efficiency of the overall system [3].

The output characteristics of photovoltaic arrays change with the cell's temperature and solar irradiance. For a given conditions there is a unique point in which the array produces maximum output power (MPPT) which varies depending of cell temperature and present irradiation level. To obtain the maximum power from a photovoltaic array, a DC-DC inverter with maximum power point tracking (MPPT) is used. In this paper we study fuzzy logic method of search for MPP.

In this paper, we study a power control of grid-connected photovoltaic system.

2. System description and simulation study

The block diagram of the complete chain: photovoltaic generator - converters - electrical network studied is given in Fig.1. A MPPT command is used to tracking the maximum power point. If the grid is disconnected the control circuits from the inverter open connection with the grid, the inverter is then supplied by the batteries to provide all the power necessary to the critical loads.

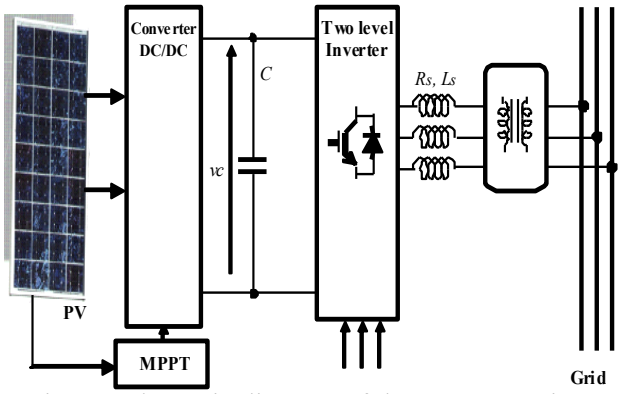

Fig. 1. Schematic diagram of the PV generation system.

3. Photovoltaic cell model

This model is the most classical one found in the literature [2] [4] [5]. As shown in Fig.2, the equivalent circuit model of a solar cell consists of a current generator (I_{ph}) and a diode plus series (R_s) and parallel

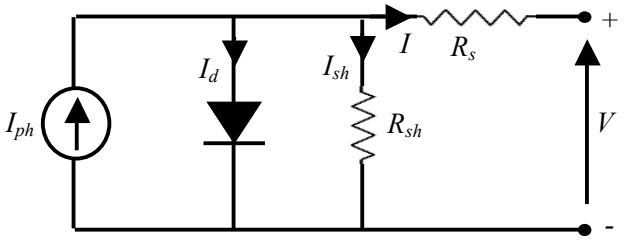

resistances (R_{sh}).

Fig. 2. Equivalent electrical circuit of a cell.

Each panel group consists of a series/parallels

association of elementary cells [6]. The photovoltaic generator shown below is thereby obtained.

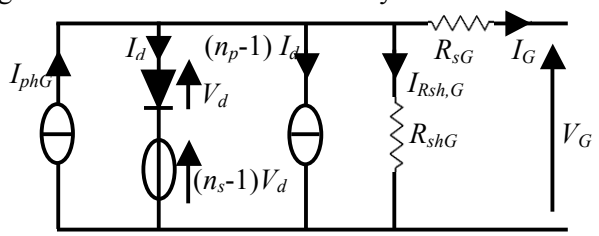

Fig. 3. Equivalent electrical circuit of a panel group.

The characteristic equation for photovoltaic panel group is deduced from the equivalent electrical diagram (Fig.3), can then be derived:

$$I_G = I_{phG} - I_{dG} - I_{shG} \quad (1)$$

The expression of the current generated by a photovoltaic cell is given by the following equation [3] [5]:

$$I_G = n_p I_{ph} - n_p I_{sc}\left(exp\left(\frac{q\left(V + IR_s\right)}{n_s nkT}\right) - 1\right) - \frac{\left(V + IR_s\right)}{R_{sh}} \quad (2)$$

With:

$$I_{sc} = I_{scref}.(T/T_0)^3.exp(-\frac{E_g}{kT}) \quad (3)$$

Fig.4 and 5 give the current–voltage (I–V) and power–voltage (P–V) characteristics of a PV module for different values of solar radiation and temperature.

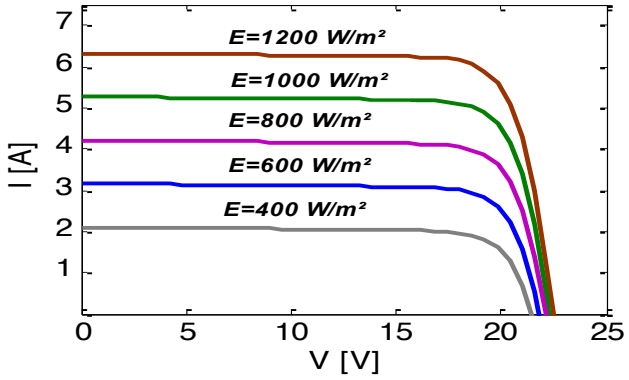

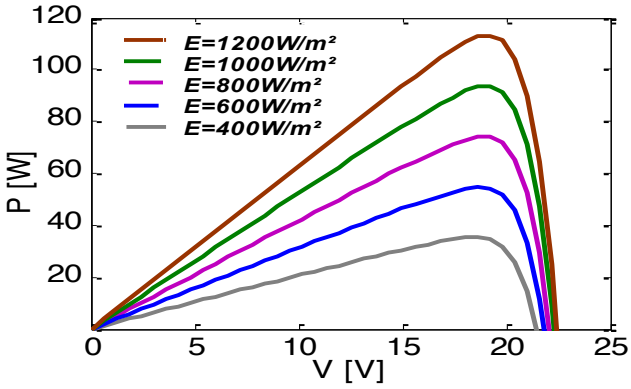

(a). Simulation case

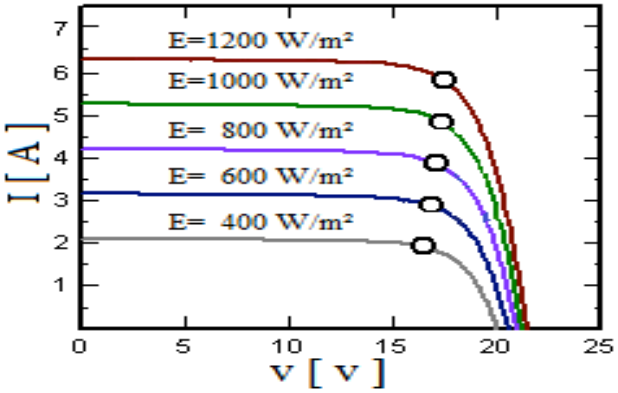

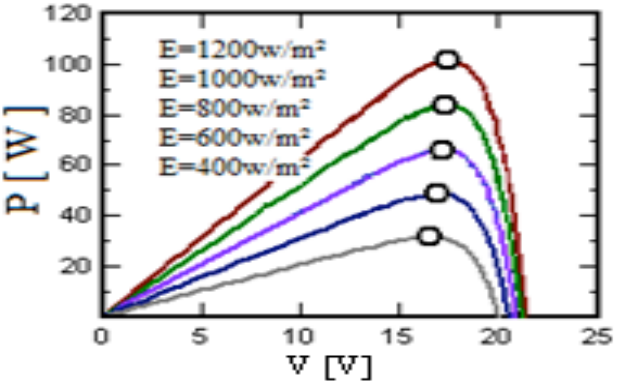

(b). Real case

Fig. 4. Effect of the irradiation on PV generator.

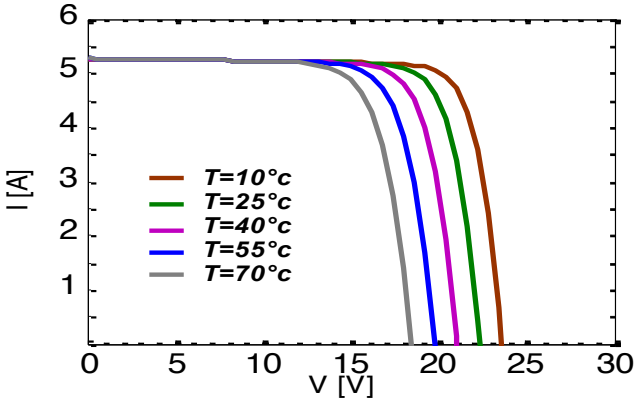

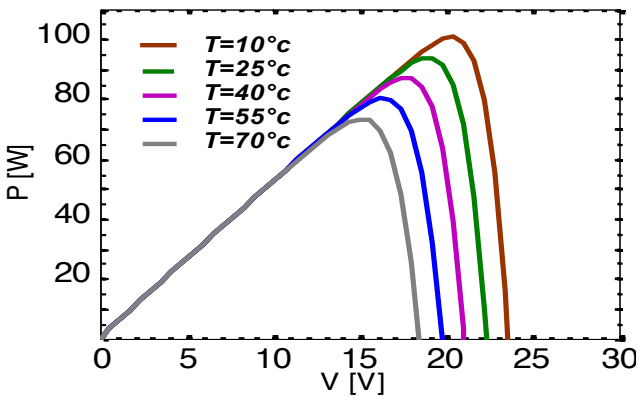

(a). Simulation case

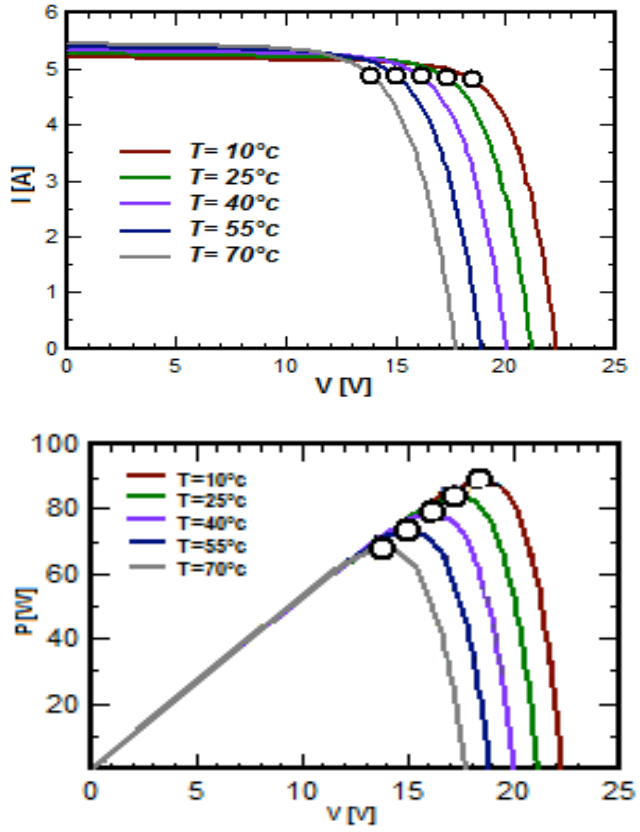

(b). Real case

Fig. 5. Effect of the Temperature on PV generator.

It is seen that the short circuit current is clearly proportional to the solar radiation (Fig.4): more radiation, more current, and also more maximum output power. On the other hand the temperature dependence is inverse (Fig.5): an increase in temperature causes a reduction of the open-circuit voltage and hence also of the maximum output power. Hence these opposite effects of the variations of solar radiation and temperature on the maximum output power make it important to track the MPP efficiently. The non-linear nature of the photovoltaic array is apparent. Thus, in order to compensate for this feature exhibited by photovoltaic arrays, a MPPT algorithm must be incorporated to force the system to always operate at the MPP resulting in high efficiency gains.

4. Buck- Boost Type DC–DC Converter

The adaptation of impedance between a photovoltaic generator and a load is a technological problem to transfer the maximum of generated power [7] [8] [9], to cure this problem we use a block of adaptation made up of a Buck-Boost converter controlled by a control circuit [10] [11].

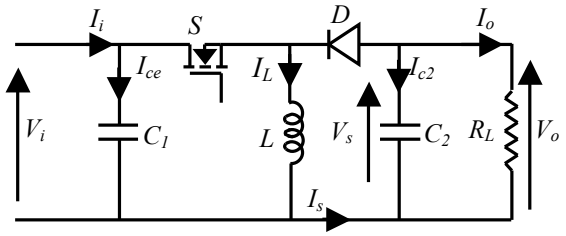

Fig. 6. Buck-Boost converter.

The approximated dynamic model of the *Buck-Boost* converter is given by the following system [7] [12]:

$$\begin{cases} I_L = \dfrac{1}{\delta}\left(I_i - C_1 \dfrac{dV_i}{dt}\right) \\ I_0 = -(1-\delta) I_L - C_2 \dfrac{dV_0}{dt} \\ V_i = \dfrac{1}{\delta}\left(-(1-\delta)V_0 + L\dfrac{dI_L}{dt}\right) \end{cases} \tag{4}$$

The expression of the conversion ratio is given as follows:

$$M(\delta) = \frac{V_o}{V_i} = \eta \frac{-\delta}{1-\delta} \tag{5}$$

Where :

$$\eta = \frac{1}{1 + \dfrac{R_L I_0}{(1-\delta)^2 V_0}} \tag{6}$$

5. Fuzzy Logic MPP Tracking controller

The maximum power that can be delivered by a photovoltaic panel depends greatly on the insulation level and the operating temperature. Therefore, it is necessary to track the maximum power point all the time [13].

Fuzzy logic controllers have the advantages of working with imprecise inputs, not needing an accurate mathematical model, and handling nonlinearity [14].

The inputs of the fuzzy logic controllers are an error E

and an error variation CE, the output is a duty cycle or its variation (Fig.7). The two fuzzy logic controllers (FLC) input variables are the error E and change of error CE at sampled times k defined by [13] [15] [16]:

$$\begin{cases} E(k) = \dfrac{P(k) - P(k-1)}{V(k) - V(k-1)} \\ CE(k) = E(k) - E(k-1) \end{cases} \quad (7)$$

Where P(k) is the instantaneous power of the photovoltaic generator.

The input E(k) shows if the load operation point at the instant k is located on the left or on the right of the maximum power point on the PV characteristic.

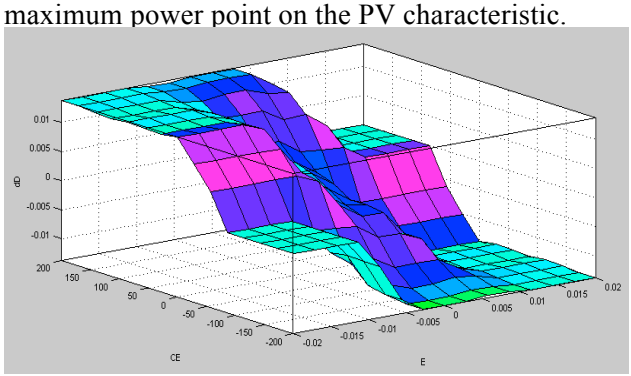

Fig. 7. Nonlinear characteristic of the optimal fuzzy controller.

During fuzzification, numerical input variables are converted into linguistic variables based on a membership function. The fuzzy inference is carried out by using Madani's method, and the defuzzification uses the centre of gravity to compute the output of this controller.

6. Modeling and control of the DC/AC inverter

The inverter control is based on a decoupled control of the active and reactive power. The DC voltage is set by a PI controller that compares the actual DC bus voltage and the reference generated by the MPPT, and provides a I_d active current reference in a synchronous reference frame attached at grid voltage vector [17]. The reactive current I_q can be fixed at the desired level for power factor or voltage control. By applying the inverse Park transformation to d-q current vector components, the desired phase current references are obtained [18] [19].

The model of the used inverter is shown in Fig. 8.

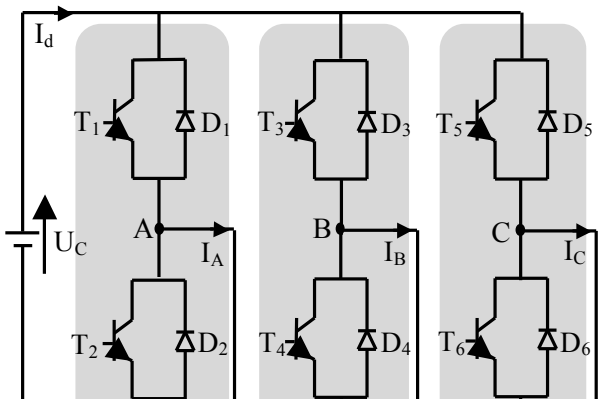

Fig. 8. Two-level inverter.

The simple output voltages at the boundaries of the load V_A, V_B and V_C are defined as follows:

$$\begin{bmatrix} V_A \\ V_B \\ V_C \end{bmatrix} = \frac{1}{3} \begin{bmatrix} 2 & -1 & -1 \\ -1 & 2 & -1 \\ -1 & -1 & 2 \end{bmatrix} . \begin{bmatrix} F_A \\ F_B \\ F_C \end{bmatrix} U_C \quad (8)$$

The figure below represents the simple tension of a phase of the two-level and its spectrum of harmonics for m=15, r=0.8 and f=50Hz.

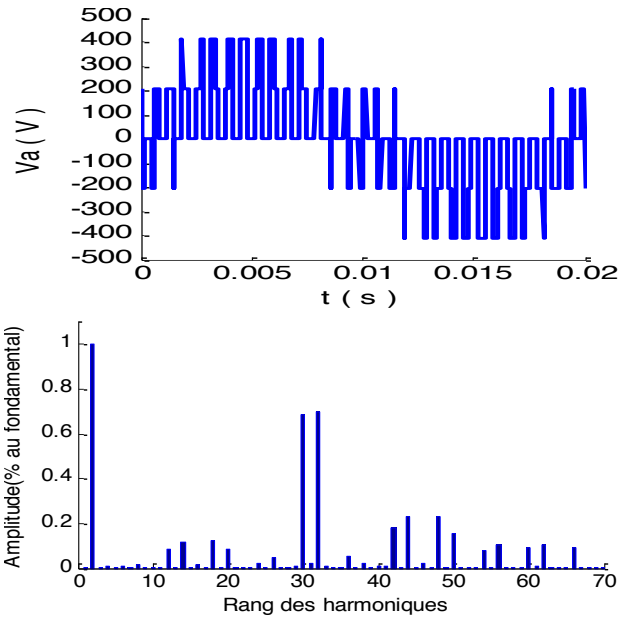

Fig. 9. Simple tension and its spectrum of the two-level.

The output voltages present symmetry relatively to the quarter of the period. The harmonics gather by families centered on frequencies multiple of *mf*. The first family centered around frequency *mf*.

7. Control the powers and the currents of the grid

7.1. Modeling and control of the grid powers

The electrical model of a phase of the electrical grid is shown in Fig.10.

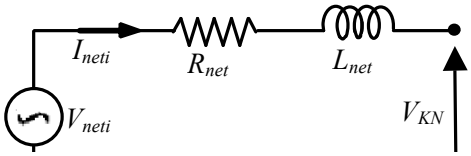

Fig. 10. Electrical model of a phase of the electrical grid.

The grid is represented by a voltage source in series with an inductance, and resistance R_{net} to attenuate the undulation of the current. Voltages grid can be given with Park components as follow [20]:

$$\begin{bmatrix} V_{dnet} \\ V_{qnet} \end{bmatrix} = \begin{bmatrix} R_{net} & -L_{net}\omega \\ L_{net}\omega & R_{net} \end{bmatrix} \cdot \begin{bmatrix} i_d \\ i_q \end{bmatrix} + \begin{bmatrix} 0 & L_{net} \\ L_{net} & 0 \end{bmatrix} \cdot \frac{d}{dt} \begin{bmatrix} i_d \\ i_q \end{bmatrix} + \begin{bmatrix} V_d \\ V_q \end{bmatrix} \quad (9)$$

Active and reactive powers can be expressed with Park components of the grid voltages and currents:

$$\begin{cases} P_g = vs_d \; is_d + vs_q \; is_q \\ Q_g = vs_d \; is_q - vs_q \; is_d \end{cases} \quad (10)$$

By inversion of these relations, it is possible to regulate the active and reactive power supply to the grid by setting the filter current references according to:

$$\begin{cases} is_{d\_ref} = \dfrac{P_{g_{ref}} . \hat{v}s_d - Q_{g_{ref}} . \hat{v}s_q}{\hat{v}_{sd}^{\,2} + \hat{v}_{sq}^{\,2}} \\ is_{q\_ref} = \dfrac{P_{g_{ref}} . \hat{v}s_q + Q_{g_{ref}} . \hat{v}s_d}{\hat{v}s_d^{\,2} + \hat{v}s_q^{\,2}} \end{cases} \quad (11)$$

Current references are gathered in a vector:

$$Is_{dq\_ref} = \left[is_{d\_ref}, is_{q\_ref} \right]^T \quad (12)$$

7.1. Control of current in the axis dq

To have good precision, we use two regulators Proportional Integral PI [21]. Their transfer function is given by:

$$H(S) = K \cdot \left(\frac{1 + T_i S}{T_i S} \right) \quad (13)$$

With:

$$K = \frac{10 \, R_{net} \, T_i}{T_e} \quad (14)$$

Where K is gain of regulator, T_i: is the integral action and T_e represents the time constant required for the current regulator.

$$T_e = \frac{L_{net}}{R_{net}} \quad (15)$$

The coupling which exists between the two currents i_d and i_q makes that the established model is very complex with the regulation. To cure this problem, we proceed to a decoupling of the two parameters by compensation, which consists in adding the terms $L_{net}\omega i_{qref}$ and $L_{net}\omega i_{dref}$ to the loop of internal regulation [22]. The control loops of the currents i_d and i_q are given by Fig.11.

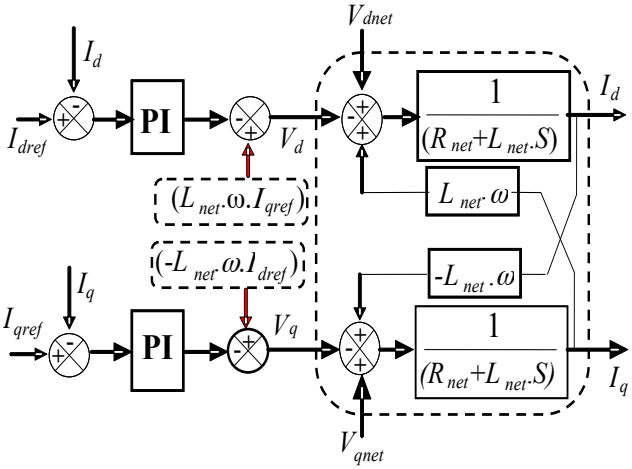

Fig. 11. Grid current control by PI regulators.

8. Simulation results

In the first section, we present the performances of photovoltaic systems connected to grid under standard test condition (E=1000W/m^2, T=25°C). The DC input voltage was set to be at 300V. The inverter is supplied by 16 series module delivering a total power P=1500W with Q = 0VAR.

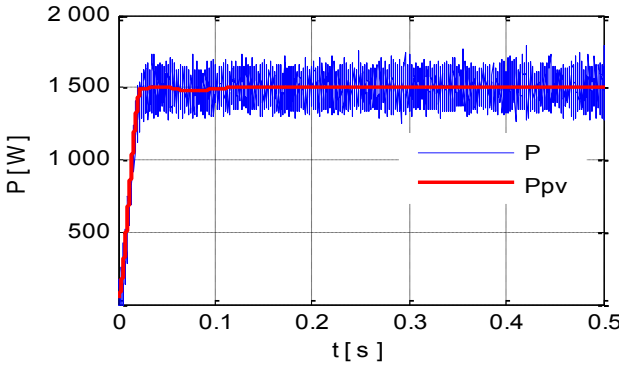

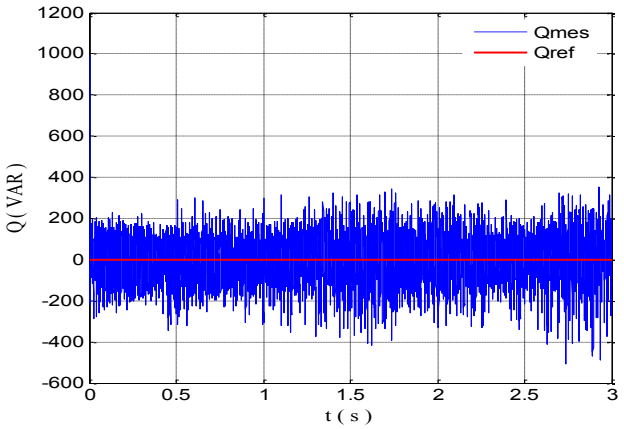

Fig. 12. Powers (active, reactive) and their references.

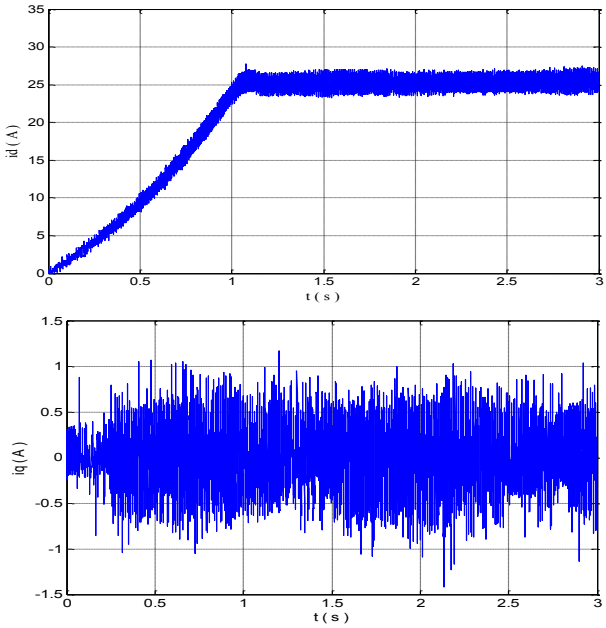

Fig. 13. Direct and quadratic current.

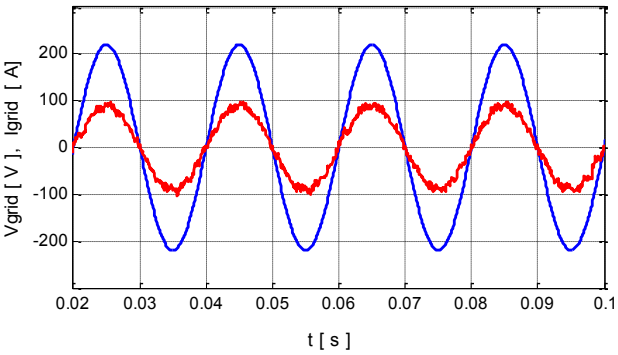

Fig. 14. Voltage and current Grid.

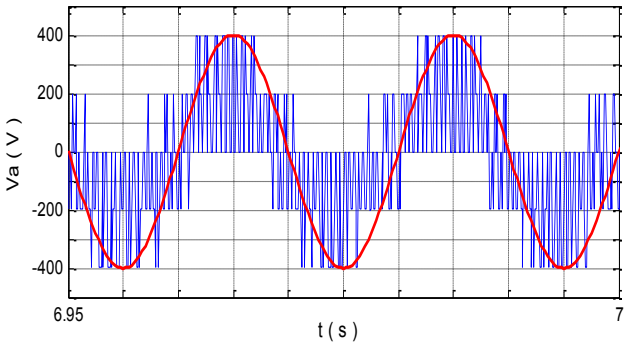

Fig. 15. Output voltage of the inverter V_A.

It is noticed that the current i_d follows the pattern of the active power P and the current i_q follows the pattern of the reactive power Q (Fig.12 and Fig.13). The photovoltaic systems have practically a unity power factor due to the fact that the grid voltage is in phase with the grid current (Fig.14). The output current of the inverter is practically sinusoidal (Fig.15).

In the second section, we study the effect of irradiance on the PV system. In the constant temperature (T=25°C), we increase the irradiance between 600W/m^2 and 1000W/m^2 during 20seconds; and after a stabilization of 10s we decrease the irradiance with the same value during also 20s.

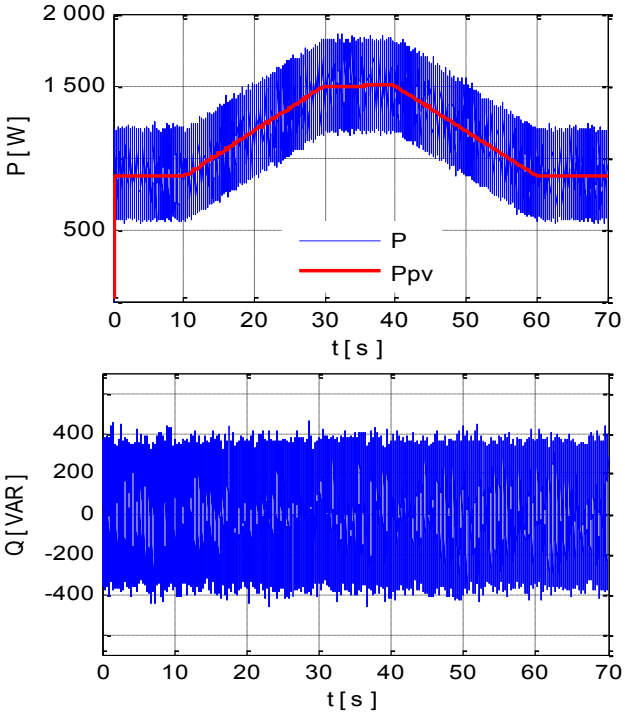

Fig. 16. Effect of irradiance variation on the active and reactive powers.

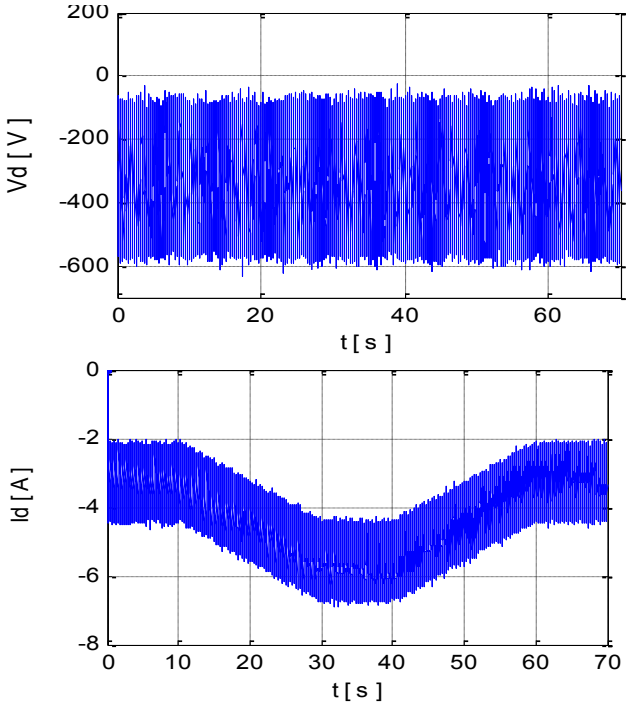

Fig. 17. Effect of irradiance variation on the direct voltage and current.

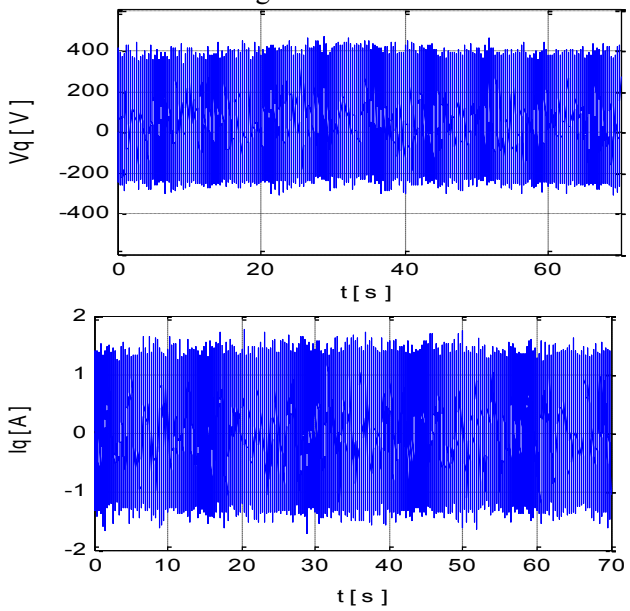

Fig. 18. Effect of irradiance variation on the quadratic voltage and current.

At the beginning, it can be seen that the photovoltaic power increase with the active power while the irradiance increases until these powers reach these maximum values which are achieved after 20 seconds of disturbance (Fig.16). The direct current i_d follows the inverse pattern of irradiance (Fig.17). The quadratic current i_q has a mean value practically equal to zero (Fig.18).

In the last section, we study the effect of temperature variation on the evolution of PV system. For a standard irradiance (E=1000W/m^2), we increase the temperature between 25°C and 75°C during 30 seconds, and after a stabilization of 20s we decrease the temperature with the same value during also 30s.

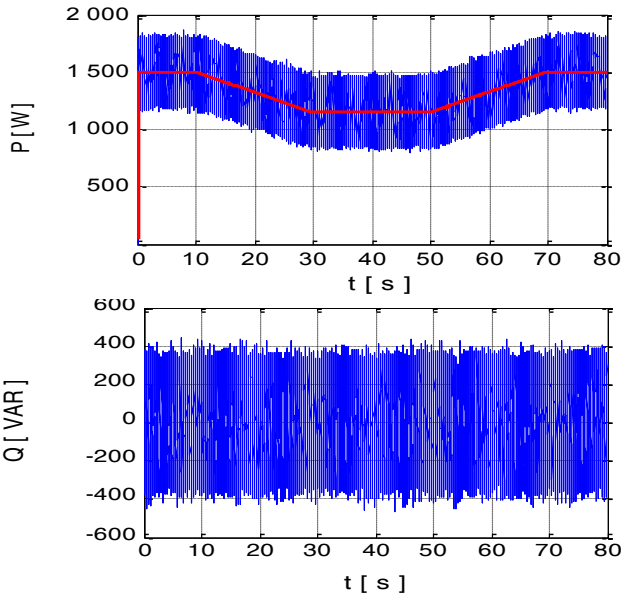

Fig. 19. Effect of temperature variation on the active and reactive powers.

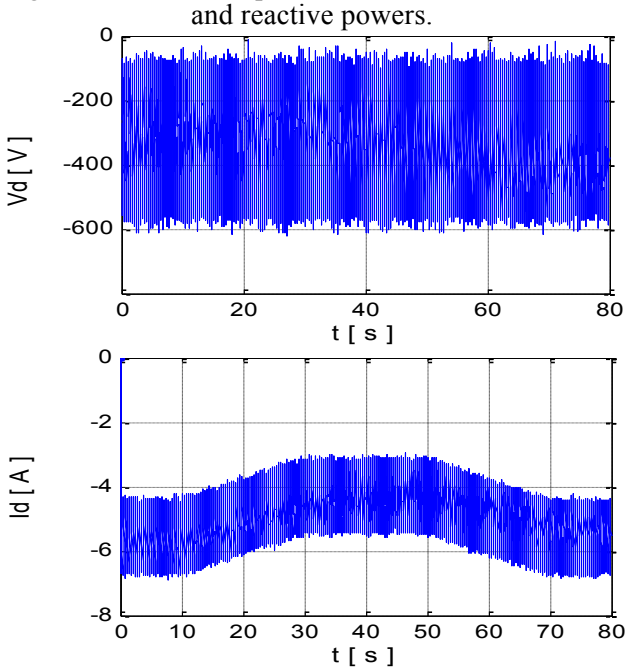

Fig. 20. Effect of temperature variation on the direct voltage and current.

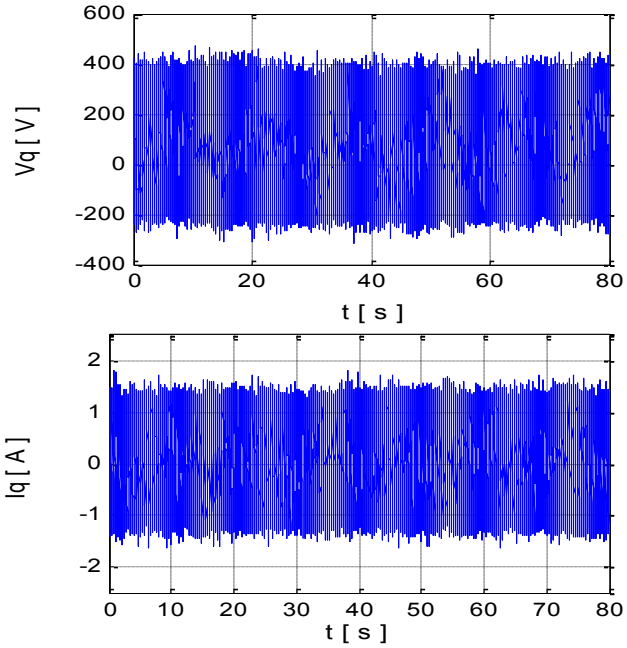

Fig. 21. Effect of temperature variation on the quadratic voltage and current.

It can be observed that the system power is inversely proportional to the temperature.

9. Conclusion

In this paper, we have studied the performances of the three phase grid connected photovoltaic system with a two levels inverter in the DC-AC stage.
Fuzzy logic MPP tracking controller is used to control the buck-boost converter in order to extract the maximum power from the photovoltaic array generator. The use of fuzzy logic controller can improve the efficiency of the overall system by minimizing the energy losses when the change of irradiation is frequent.

The entire photovoltaic generation system has been numerically simulated. Simulation results in both steady state and dynamic conditions have been presented. The results show good performance of the control system and confirm the effectiveness of the proposed photovoltaic generation system for any operating condition.

References

1. Aly M., Eid A., Mamdouh A.: *Advanced Modeling of Photovoltaic Energy Systems for Accurate Voltage Stability Assessment of Distribution Systems*. Advanced Science Letters, Vol. 19, No. 5, 2013, p. 1353-1357.
2. Ikegami T., Maezono T., Nakanishi F., Yamagata Y., Ebihara K.: *Estimation of equivalent circuit parameters of PV module and its application to optimal operation of PV system*. Solar Energy Materials & Solar Cells, Vol. 67, No. 1, 2001, p. 389-395.
3. Kolhe M.: *Techno-Economic Optimum Sizing of a Stand-Alone Solar Photovoltaic System*. IEEE Transactions on Energy Conversion, Vol. 24, No. 2, 2009, p. 511-519.
4. Siddiquia M.U, Arifa A.F.M., Biltonb A.M., Dubowskyb S., Elshafeic M.: *An improved electric circuit model for photovoltaic modules based on sensitivity analysis*. Solar Energy, Vol. 90, 2013, p. 29-42.
5. El Shahat A.: *PV Cell Module Modeling & Ann Simulation For Smart Grid Applications*. Journal of Theoretical and Applied Information Technology, Vol. 16, No. 1, 2010, p. 9-20.
6. Merten J., Asensi J.M., Voz C., Shah A.V., Platz R., Andreu J.: *Improved Equivalent Circuit and Analytical Model for Amorphous Silicon Solar Cells and Modules*. IEEE Transactions on Electron Devices, Vol. 45, No. 2, 1998, p. 423-429.
7. Enslin J.H.R., Wolf M.S., Snyman D.B., Swiegers W.: *Integrated photovoltaic maximum power point tracking converter*. IEEE Transaction on Industrial Electronics, Vol. 44, No. 6, 1997, p. 769-773.
8. Geoffrey R.W., Sernia P.C.: *Cascaded DC–DC Converter Connection of Photovoltaic Modules*. IEEE Transactions on Power Electronics, Vol. 19, No. 4, (2004), p. 1130-1139.
9. Ghaisari J., Habibi M., Bakhsahi A.: *An MPPT Controller Design for Photovoltaic (PV) System Based on the Optimal Voltage Factor Tracking*. IEEE Canada electrical Power Conference, 2007, p. 359-362.
10. Pandey A., Dasgupta N., Mukerjee A.K.: *A Single-Sensor MPPT Solution*. IEEE Transaction on Power Eletronics, Vol. 22, No. 2, 2007, p. 698-700.
11. Sokolov M., Shmilovitz D.: *A modified MPPT Scheme for Accelerate Convergence*. IEEE Transactions on Energy Conversion, Vol. 23, No. 4, 2008, p. 1105-1107.
12. Peftitsis D., Adamidis G., Bakas P., Balouktsis A.: *Photovoltaic system MPPTracker Investigation and implementation using DSP engine and buck-boostDC-DC converter*. IEEE Power Electronics and Motion Control Conference, 13th EPE-PEMC, September 1-3, 2008, Poznań, Poland, p. 1840-1846.
13. Talha A., Boumaaraf H., Bouhali O.: *Evaluation of maximum power point tracking methods for photovoltaic systems*. Archives of Control Sciences, Vol. 21, No. 2, 2011, p. 151-165.
14. Veerachary M., Senjyu T., Uezato K.: *Feedforward maximum power point tracking of PV systems usingfuzzy controller*. IEEE transactions on Aerospace and Electronics Systems, Vol. 38, No. 3, 2002, p. 969-981.
15. Chin C.S., Neelakantan P., Yoong H.P., Teo K.T.K.: *Fuzzy Logic Based MPPT for Photovoltaic Modules Influenced bySolar Irradiation and Cell Temperature*. In: Proceedings of the 13th International Conference on Modelling and Simulation UKSim'2011, 30 March - 1 April, 2011, Cambridge University (Emmanuel College), p. 376-381.
16. Tafticht T. et al: *An improved maximum power point tracking method for photovoltaic systems*. Renewable Energy, Vol. 33, No. 7, 2008, p. 1508-1516.
17. Rebei N., Ben Ghanem B., Hasnaoui O.: *Modeling and control of photovoltaic energy conversion connected to the grid*. Frontiers in Energy, 6, No. 1, 2012, p. 35-46.
18. Blaabjerg F., Chen Z., Kjaer S.: *Power electronics as efficient interface in dispersed power generation systems*. IEEE Transactions on Power Electronics, Vol. 19, No. 5, 2004, p. 1184-1194.
19. Cecati C., Dell'Aquila A., Liserre M.: *A novel three-phase singlestage distributed power inverter*. IEEE Transactions on Power Electronics, Vol. 19, No. 5, 2004, p. 1226-1233.
20. Seul-Ki K., Jin-Hong Jeon J., Chang-Hee C., Jong-Bo

A., Sae-Hyuk K.: *Dynamic Modeling and Control of a Grid-Connected Hybrid Generation System With Versatile Power Transfer*. IEEE Transactions on Industrial Electronics, Vol. 55, No. 4, 2008, p. 1677-1688.
21. Salhi M., El-Bachtiri R.: *A Maximum Power Point Tracking Photovoltaic System using a Proportional Integral Regulator*. Science Academy Transactions on Renewable Energy Systems Engineering and Technology, 1, No. 2, 2011, p. 38-44.
22. D. N. Zmood, D.G. Holmes: Stationary Frame Current Regulation of PWM Inverters with Zero Steady-State Error. IEEE Transaction on Power Electronics, Vol. 18, No. 3, 2003, p.814-822.